

2023

# TSP-1 reduced the size of episcleral veins

---

<https://hdl.handle.net/2144/47449>

*Downloaded from OpenBU. Boston University's institutional repository.*

BOSTON UNIVERSITY

ARAM V. CHOBANIAN & EDWARD AVEDISIAN SCHOOL OF MEDICINE

Thesis

**TSP-1 REDUCED THE SIZE OF EPISCLERAL VEINS**

by

**ABID KHAN**

B.S., Northeastern University, 2020

Submitted in partial fulfillment of the  
requirements for the degree of

Master of Science

2023



Approved by

First Reader

---

Haiyan Gong, M.D., Ph.D.  
Professor of Ophthalmology, Anatomy and Neurobiology

Second Reader

---

Andrew Taylor, Ph.D.  
Professor of Ophthalmology

## **DEDICATION**

I would like to dedicate this work to my family who have supported me throughout my journey and academic career. My parents, Rumana and Rehan, played an intricate role into shaping me into who I am to this day. I also would like to dedicate this work specifically to my 93-year-old grandfather, as he is someone who inspires me with every passing day. Finally, my three siblings who have held me accountable deserve recognition for keeping me on track.

## **ACKNOWLEDGMENTS**

I would like to acknowledge those who are a part of the Gong Lab. Specifically Dr. Gong and Flora, who both took the time to introduce me to the lab and get me situated. They put me in a place to be successful during this research. I would also like to thank Neil for taking the time to train me when I started, Hoilam Li for the assistance of statistical analysis, as well as Shayna who was there to answer any questions that I might have had.

## **TSP-1 REDUCED THE SIZE OF EPISCLERAL VEINS**

**ABID KHAN**

### **ABSTRACT**

**Introduction and Aim:** Primary Open-Angle Glaucoma (POAG) is a leading cause of blindness worldwide. The pathology is characterized by elevated resistance to aqueous humor (AH) outflow which leads to an increased intra-ocular pressure (IOP). Elevated IOP is a risk factor for the development and progression of POAG because increased IOP can cause visual impairments or blindness by damaging the optic nerve. Previous studies indicated that Thrombospondin-1 (TSP-1) expression is higher in glaucomatous eyes and TSP1-deficient mice exhibit lowered IOP, suggesting TSP-1 plays a role in regulating IOP. A preliminary study in the Gong Lab has showed that TSP-1 decreased outflow facility in porcine eyes. This study aims to explore morphologic changes in the trabecular meshwork and episcleral veins (ESVs) in porcine eyes that were previously treated with either TSP-1 or phosphate-buffered saline containing 5.5 mM D-glucose (GPBS).

**Methods:** Nine fresh porcine eyes were used in this study. All eyes were perfused with GPBS for 30 minutes to establish a stable baseline outflow facility. TSP-1 (0.8µg/mL) was then exchanged and perfused to one eye of each pair for 3 hours, while GPBS was exchanged and perfused to the contralateral eyes (N=5) as the control group. All perfusion was performed at a consistent pressure of 15mmHg, and the outflow facility was recorded. After perfusion, all eyes were perfused with a fluorescent tracer to label the

outflow pattern, and then they were perfusion-fixed. The tissue of the anterior chamber angle of each eye was dissected and processed for light microscopy. One TSP-1 treated eye was excluded for morphologic study due to damage of the tissue. Three wedges from each eye were used for data collection and analysis. Semi-thin sections of each sample were cut and stained with 0.1% Toluidine Blue. The morphology of trabecular meshwork was evaluated. Numbers of episcleral veins (ESVs) were counted and their sizes (cross-sectional areas) were measured using ImageJ (NIH). This study was masked and decoded after all the measurements were done. Statistical significance between control and TSP-1 treated was analyzed.

**Results:** Outflow facility was significantly decreased in the TSP-1 treated group compared to the control group (performed by other members in Gong lab). The average cross-sectional area of ESVs ( $797.0 \pm 30.1 \mu\text{m}^2$ ) in the TSP-1 treated group was significantly smaller than the area of ESVs ( $1628.2 \pm 191.3 \mu\text{m}^2$ ) in the control group ( $P < 0.05$ ). No significant morphologic differences were found in the TM of TSP-1 treated eyes when compared to the control.

**Conclusions:** TSP-1 reduced the size (cross-sectional area) of ESVs, which may contribute to decreased outflow. The findings of this study suggest that blocking TSP1-induced vasoconstriction in the ESVs could be a potential target to increase outflow facility or lower IOP for glaucoma treatment.

## **PREFACE**

Glaucoma is one of the leading causes of blindness worldwide. To this day, the disease is not completely understood. The work of Dr. Haiyan Gong's lab has contributed to literature over the years. This project will hopefully add to literature regarding glaucoma research and furthermore contribute to the development of novel therapeutics that have a positive impact on patients with glaucoma. Adding to prior knowledge and literature regarding glaucoma, and more specifically Primary Open-Angle Glaucoma, could prove to be impactful in the future. This project has opened my eyes to the field of ophthalmology and has really captivated my interests in research.

## TABLE OF CONTENTS

DEDICATION .....	iv
ACKNOWLEDGMENTS.....	v
ABSTRACT .....	vi
PREFACE .....	viii
TABLE OF CONTENTS .....	ix
LIST OF TABLES .....	xi
LIST OF FIGURES.....	xii
LIST OF ABBREVIATIONS .....	xiii
CHAPTER ONE - INTRODUCTION .....	1
1.1 - Prevalence of Glaucoma .....	1
1.2 - Elevation of IOP is a Major Risk Factor for POAG .....	1
1.3 - Aqueous Humor Outflow.....	2
1.4 - Porcine Eyes vs. Human Eyes.....	8
1.5 - TSP-1 and Prior Studies from Gong Lab .....	11
1.6 - TSP-1 Decreased Outflow Facility .....	12
1.7 - Goal of this Study .....	15
CHAPTER TWO - EXPERIMENTAL DESIGN AND METHODS .....	16
2.1 - Tissue Preparation.....	16
2.2 - Sectioning and Staining for Light Microscopy .....	16
2.3 - Imaging .....	17
2.4 - Methods of Data Analysis.....	20

CHAPTER THREE - RESULTS .....	226
3.1 - Grouping of Eyes .....	26
3.2 - Comparison of Average ESV Area between Control and TSP-1 Treated Eyes....	26
3.3 - Comparison of Trabecular Meshwork Morphology between TSP-1 Treated and Control Groups.....	30
CHAPTER FOUR - DISCUSSION .....	33
BIBLIOGRAPHY .....	37
CURRICULUM VITAE .....	42

**LIST OF TABLES**

Table 3.2. **Comparison of average *ESV* area between control and TSP-1 treated groups**  
.....27

## LIST OF FIGURES

Figure 1.1 - <i>A cartoon illustration of the conventional outflow pathway</i> .....	4
Figure 1.2 - <i>AH flows through layers of the TM</i> .....	6
Figure 1.3 - <i>A LM image of outflow pathway in human eye</i> .....	7
Figure 1.4 - <i>Histology of Anterior Segment of Porcine Eye</i> .....	10
Figure 1.5 - <i>TSP1 decreases outflow facility in porcine eyes</i> .....	14
Figure 2.1 - <i>ESVs vs ESAs</i> .....	19
Figure 2.2 - <i>An Example of an ESV</i> .....	21
Figure 2.3 - <i>Calibration slide</i> .....	23
Figure 2.4 - <i>Example of how ESVs were traced</i> .....	24
Figure 3.1 - <i>Unpaired t-test was performed for unpaired ESV area</i> .....	28
Figure 3.2 - <i>Paired t-test was performed for paired normalized ESV</i> .....	29
Figure 3.3 - <i>TM Images</i> .....	31

## LIST OF ABBREVIATIONS

AH.....	Aqueous Humor
AP.....	Aqueous Plexus
ECM.....	Extra-Cellular Matrix
ESV.....	Episcleral Vein
IOP.....	Intra-Ocular Pressure
JCT.....	Juxtacanalicular Tissue
NO.....	Nitric Oxide
POAG.....	Primary Open-Angle Glaucoma
SC.....	Schlemm's Canal
TM.....	Trabecular Meshwork
TSP-1.....	Thrombospondin-1

## CHAPTER ONE – INTRODUCTION

### 1.1 Prevalence of Glaucoma

Primary open-angle glaucoma (POAG) is the second-leading cause of blindness worldwide (Weinreb et al., 2014). Glaucoma can lead to permanent bilateral blindness, and it affects more than 70 million people worldwide. (Weinreb et al., 2014) Experts say that the number of people affected by glaucoma is underreported worldwide, and that many people do not even know that they have it. (Weinreb et al., 2014) As a result, the actual prevalence of glaucoma could be significantly higher than what is known.

### 1.2 Elevation of IOP is a Major Risk factor for POAG

Elevated IOP is considered to be the main risk factor for the development and progression of POAG. (Boland et al., 2007) Data in recent years has shown there to be a definite correlation between increased IOP and POAG pathogenesis. (Noecker et al., 2006) Ocular hypertension over time results in damage to the optic nerve along with symptoms of visual field deficiencies, which ultimately can lead to blindness if left untreated. (Boland et al., 2007) Reduction in IOP is the only proven method of treating patients with POAG. (Weinreb et al., 2014) As a result, much of the current research focuses on the development of therapeutics that will reduce IOP. Therapeutics relevant to the treatment of POAG include pharmacologic interventions, surgical interventions, and laser-surgery that aim to reduce IOP. (Sihota et al., 2018) Lowering IOP can prevent the

development and progression of POAG and could help prevent patients from going blind. (Sihota et al., 2018)

Other than the elevation of IOP, other contributing risk factors include increasing age, genetic and hereditary components, race and ethnicity, central corneal thickness, complications resulting from other systemic diseases, and others. (Boland et al., 2007) A previous study conducted by the Gong Lab compared n=20 normal eyes to n=20 POAG eyes by measuring scleral spur length and percentage of Schlemm's Canal (SC) collapse. Findings from this study suggest that having a shorter scleral spur length can cause a collapse of the SC and could be a risk factor for the development of POAG. (Swain et al., 2015) While the elevation of IOP is the primary risk factor for the development of POAG, other contributing factors are associated, suggesting that POAG is a multifactorial disease.

### **1.3 Aqueous Humor Outflow**

Aqueous humor (AH) is a fluid secreted by the ciliary body that contains nutrients such as electrolytes, growth factors, proteins. The AH provides nutrition to the anterior segment of the eye and to the avascular cornea and lens. It is essential for the normal maintenance and physiology of the ocular microenvironment. AH enters the posterior chamber after produced by the ciliary body, then it flows through the pupil into the anterior chamber. (Goel et al., 2010) AH flows out of anterior chamber through two pathways: the conventional outflow pathway and unconventional pathway. (Goel et al.,

2010) The majority of AH drains through the conventional trabecular pathway. (Jingna et al., 2022) IOP is maintained in a normal range through the dynamic balance between aqueous humor production and drainage. Elevated IOP in POAG is associated with increased resistance in the trabecular outflow pathway. (Abu-Hassan et al., 2014) An overview of the anatomy of the conventional (trabecular) outflow pathway is shown in **Figure 1.1** below:

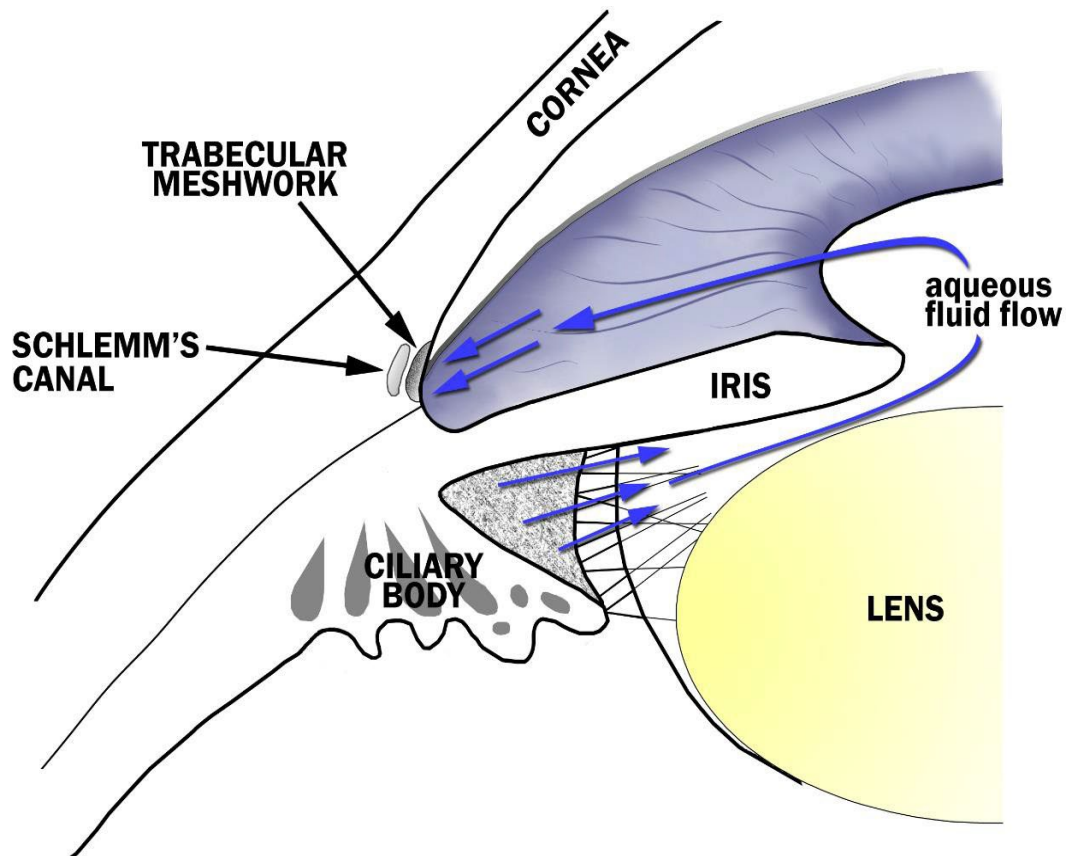


**Figure 1.1** – *A cartoon illustration of the conventional outflow pathway. The blue arrows represent how AH flows throughout the conventional outflow pathway. Structures involved in secretion and drainage of AH are labelled with black arrows. The ciliary body secretes AH, which eventually flows through the trabecular meshwork and into Schlemm’s canal, which drains into episcleral veins (not shown). (From “The Glaucoma Eye”, 2022.)*

In the conventional outflow pathway, AH flows into a layered structure known as the trabecular meshwork (TM). The TM is a structure containing beams. Each beam is made of a connective tissue core containing collagen, elastic fiber and proteoglycans covered by endothelial cells (Gong et al., 1996). The trabecular meshwork can be divided into different regions: the uveal meshwork, corneoscleral meshwork, and the juxtacanalicular tissue (JCT). The JCT is also referred to as the cribiform meshwork. AH traverses through the different layers of the TM prior to reaching the inner wall of SC. The flow of AH through the layers of TM is depicted below:

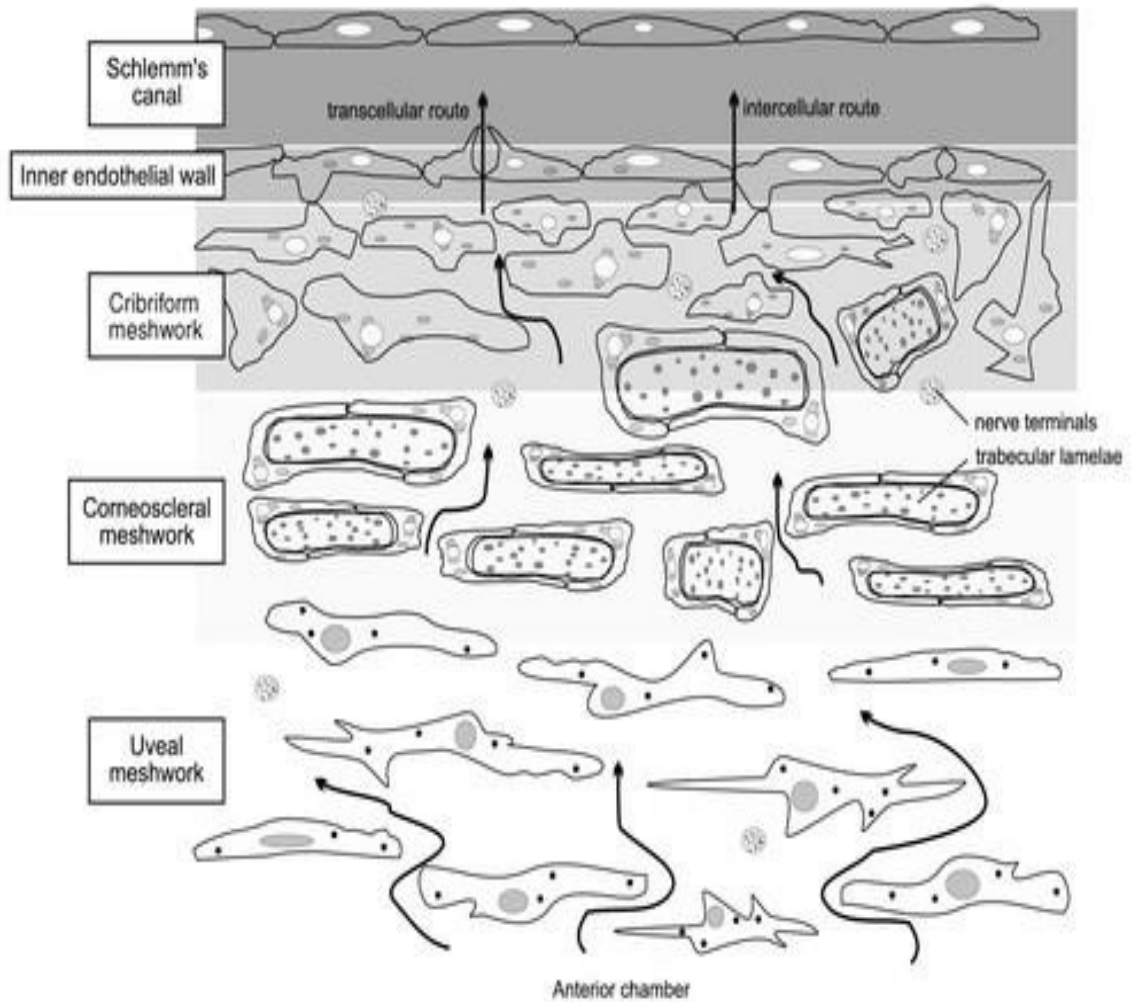


**Figure 1.2 – AH flows through layers of the TM.** This illustration depicts the flow of AH through the different layers of the TM before it reaches the inner wall of SC. The black arrows represent AH flowing in the TM throughout the inter-trabecular spaces. (From Llobet et al., 2003)

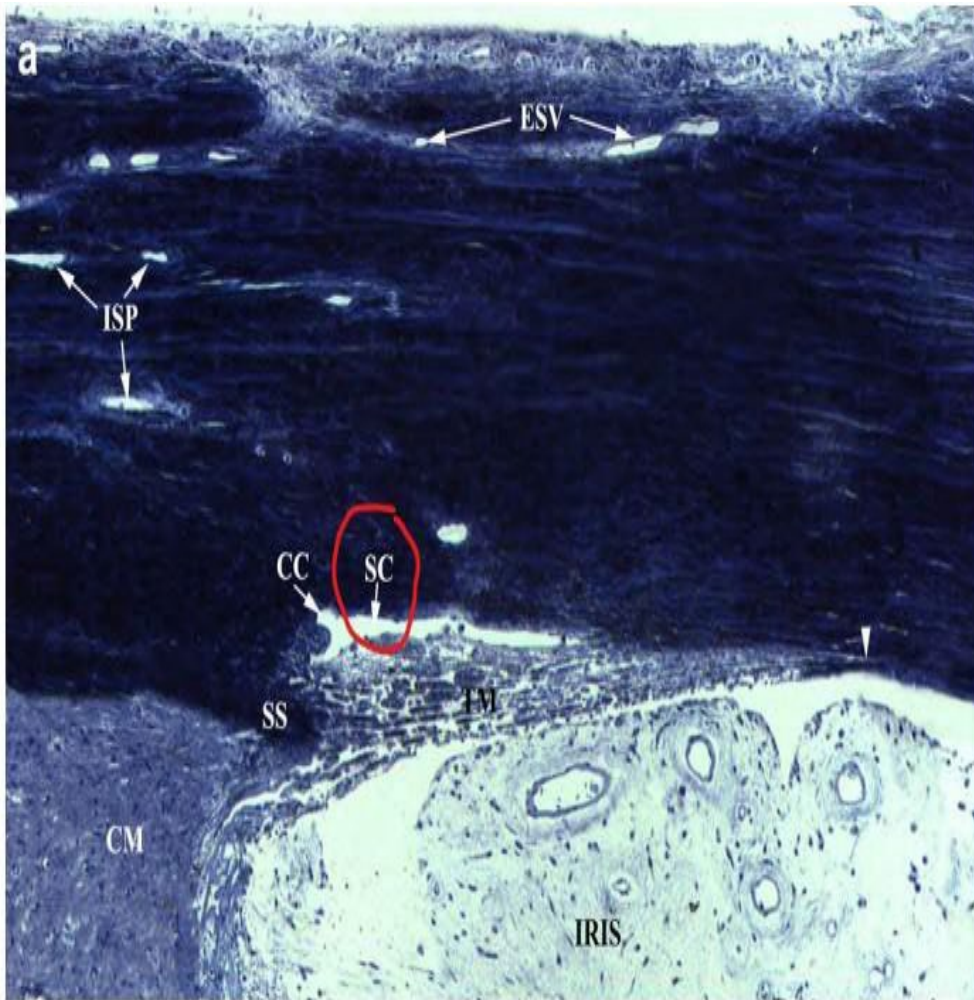


**Figure 1.3** – *A light microscopic image of outflow pathway in human eye. This figure shows the important structures along the trabecular outflow pathway, which are the ciliary muscle (CM), scleral spur (SS), collector channel (CC), intrascleral plexus (ISP), and episcleral veins (ESV). (From Gong & Swain, 2020)*

The conventional outflow pathway of a human eye under light microscope was showed in **Figure 1.3**. The image was adapted from Dr. Haiyan Gong, and morphologies involved in the outflow pathway are labeled. (Gong et al., 2020)

In cases of glaucoma, the conventional outflow pathway can be hindered at any point or at multiple points along the pathway. For example, there can be increased resistance to AH flow through the different layers of the TM. (Llobet et al., 2003) When there is an increase in resistance to outflow, this causes a build-up of AH leading to elevated IOP and to the pathogenesis of POAG. (Boland et al., 2007) Increased IOP results in the destruction of optic nerve fibers that is seen as a narrowing of the neuroretinal rim of the optic nerve head with enlargement of the central cup of the optic nerve head. (Webers et al., 2008) Progression of POAG leads to irreparable blindness because of increased IOP impacting the number of viable axons within the optic nerve.

#### **1.4 Porcine eyes vs. Human eyes**

This study focuses on the morphologic effects of TSP-1 on ESVs and TM using porcine eyes. The anatomy of porcine eyes differs from human eyes only slightly. Porcine eyes do not contain a single SC. (McMenamin et al., 1991) Instead, a series of channels known as the aqueous plexus (AP) are found. Despite this, the conventional aqueous outflow pathway follows the same pattern of that of human eyes. (McMenamin et al., 1991) Furthermore, there are anatomical and morphological similarities between

porcine eyes and human eyes. The anterior chamber of porcine eyes is similar in size and volume to that of humans. (McMenamin et al., 1991) In addition, porcine eyes have a similar sized mass of corneoscleral tissue found within the scleral sulcus when compared to the human trabecular meshwork. (McMenamin et al., 1991) Porcine eyes are readily available and cheap. As a result, porcine eyes are used in this study. While **Figure 1.4** is a representation of the conventional outflow pathway of the porcine eye, it should be noted that the aqueous plexus (AP) is sometimes also referred to as Schlemm's canal like structure (SCLS). (Dang et al, 2018)

# Control

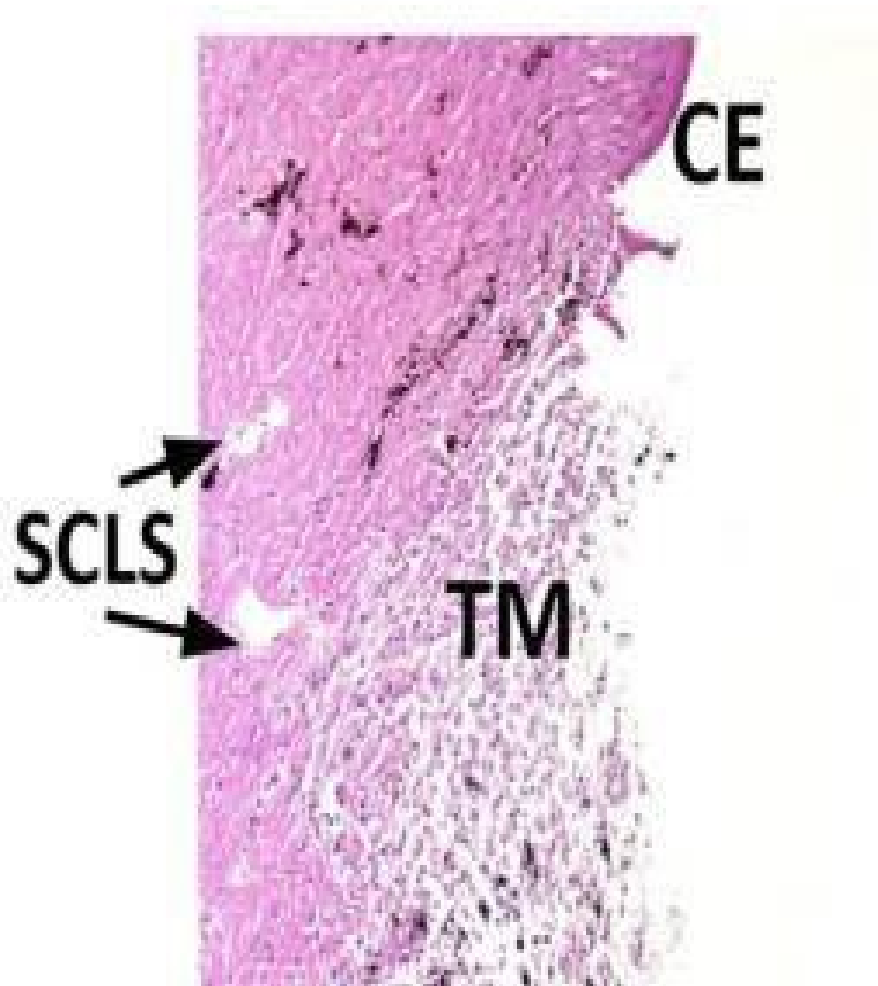


**Figure 1.4 – Histology of Anterior Segment of Porcine Eye.** This figure represents the anterior segment of a porcine eye taken from a prior study (Dang et al., 2018). The trabecular meshwork is labelled TM, and the aqueous plexus is labelled (arrows) as Schlemm's canal like structure (SCLS). (Dang et al., 2018)

### **1.5 TSP-1 and Prior Studies from Gong Lab**

Thrombospondin-1 (TSP-1) is a glycoprotein that interacts with cell adhesion receptors and growth factors in the extra-cellular matrix (ECM). (Flügel-Koch et al., 2004) TSP-1 is involved in platelet aggregation, angiogenesis, and cell growth. One function of TSP-1 is the activation of Latent-Transforming Growth Factor – beta (LTGF- $\beta$ 2). Activated TGF- $\beta$  regulates cell proliferation, and the production of cytokines and structural components of the ECM. (Murphy-Ullrich et al., 2015) TSP-1 has been found in the TM, and the level of TSP-1 present in the TM increases with age. (Murphy Ullrich et al., 2015) Past studies have demonstrated that upregulated activation of TGF- $\beta$  is associated with the induction of POAG. Therefore it has been suggested that the upregulation of TGF-b activation is caused by enhanced expression of TSP-1 and that this leads to the pathogenesis of POAG. (Murphy Ullrich et al., 2015) Therefore the role of TSP-1 in the regulation and modification of morphologies in the TM would have an impact on aqueous humor outflow resistance, and thus elevate IOP leading to glaucoma.

The eyes of six glaucoma patients (including one with steroid-induced glaucoma) were found to have “intense” TSP-1 immuno-reactivity with positive labelling throughout the entire TM in a previous study. Additionally, this study assessed mRNA expression of TSP-1 in both fresh and cultured TM cells. Incubation of TM cells with TGF- $\beta$ 1 and dexamethasone caused a marked increase in TSP-1 expression. These findings suggest that TSP-1 in the TM might act as a potent local endogenous activator of TGF- $\beta$ s in the

aqueous humor, and TSP-1 could also mediate local effects of TGF- $\beta$  and/or dexamethasone on the outflow of AH. (Flügel-Koch et al., 2004)

Another study assessed the effects of TSP-1 on IOP. Comparison of eyes from TSP-1 knocked out mice to eyes from wild-type (WT) mouse eyes demonstrated that the average IOP for the TSP-1 knockout eyes is  $14.2 \pm 2.0$  mmHg, while the average IOP of the WT eyes is  $15.8 \pm 1.5$  mmHg. This study found that TSP-1 deficient mouse eyes exhibited a statistically significant 10% lower IOP. (Haddadin et al., 2012) The results suggest that TSP-1 expression plays a role in the regulation of IOP.

Similarly, another study conducted in the Gong lab used TSP-1 knockout mice (n=14) and wild-type (WT) mice (n=14) to investigate the difference in steroid (dexamethasone)-induced ocular hypertension. (Ren & Gong, 2021) The results showed that steroid- induced elevation of IOP is delayed, and the peak elevation of IOP is reduced but is not sustained in TSP-1 deficiency mice compared to WT mice. (Ren & Gong, 2021) This further supports the potential for TSP1 to play a role in regulating IOP.

### **1.6 TSP-1 Decreased Outflow Facility**

Prior studies in the Gong lab assessed outflow facility in porcine eyes when the eyes are perfused with either GPBS or TSP-1 for 3 hours. In normal porcine eyes, as perfusion continues the outflow facility of the eye progressively increases, which is called the washout effect. The morphological correlation with the washout effect is the separation of the connections between the JCT cell/matrix and inner wall.

(Gong et al., 2009, Scott et al., 2009) When compared to normal control eyes, TSP-1 perfused porcine eyes do not experience the washout effect (Figure 1.5 below).

After 1-, 2- and 3-hour measurements, the outflow facility of TSP-1 is significantly lower than the control eyes for  $0.03 \pm 0.02 \mu\text{l/ min/ mmHg}$  (10%,  $P < 0.01$ ),  $0.04 \pm 0.02 \mu\text{l/ min/ mmHg}$  (15%,  $P < 0.0001$ ) and  $0.05 \pm 0.02 \mu\text{l/ min/ mmHg}$  (16%,  $P < 0.0001$ ) respectively.

These results demonstrate that the outflow facility is significantly decreased in TSP-1 treated eyes at 1, 2 and 3 hours compared to control eyes. However, the morphologic changes that may contributed to the decrease in outflow facility has not been investigated.

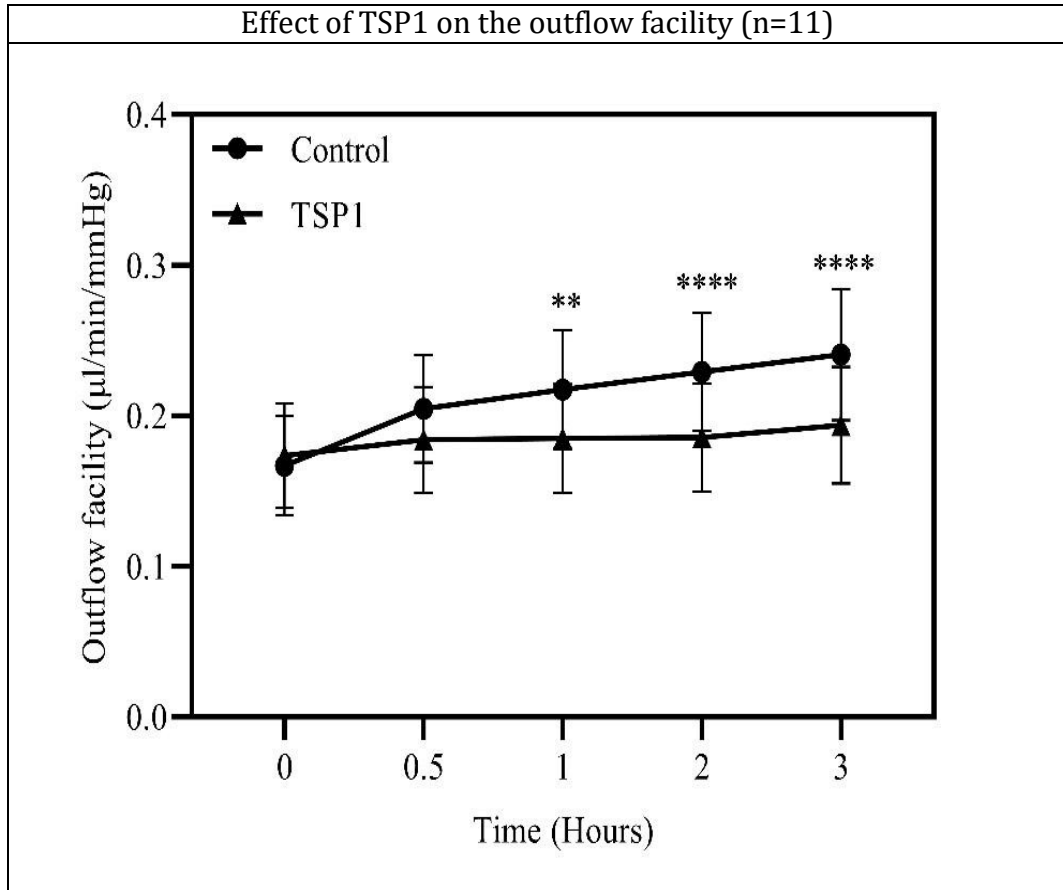


**Figure 1.5 – TSP1 decreases outflow facility in porcine eyes (n=11 pairs)**

*This figure is provided by Dr. Gong from a previous study conducted in the Gong Lab, demonstrates that outflow facility is significantly decreased in TSP-1 treated eyes when compared to control eyes. A two-way repeated measurement ANOVA with a Bonferroni's multiple comparisons test was used for the post hoc test. \*\* $P < 0.01$ ; \*\*\* $P < 0.001$ ; \*\*\*\* $P < 0.0001$ . Average  $\pm$  SEM was presented in the graph for 11 pairs of porcine eyes.*

### **1.7 Goal of this study**

The goal of this study is to assess morphologic changes in the outflow pathways including trabecular meshwork and episcleral veins in porcine eyes that were either perfused with TSP-1 or GPBS (Facility data was shown in figure 1.5 above). The results of this investigation could provide insight into the relationship between the structure changes in the outflow pathway and decreased outflow facility by TSP-1 treatment.

## CHAPTER TWO – EXPERIMENTAL DESIGN AND METHODS

### **2.1 Tissue Preparation**

Ten porcine eyes (5 pairs) without knowing previous treatment with either TSP-1 (experimental) or GBPS (control) were used in this study. The eyes were perfusion-fixed with modified Karnovsky's fixative (2.5% glutaraldehyde and 2% paraformaldehyde, pH 7.3), and the eyes were perfusion-fixed at 15 mmHg for 30 min. After perfusion was completed, a small cut was made along the equator, and each eye was immersed in the same fixative for 24 hours.

Each eye was dissected into the anterior and posterior segments. The anterior segment of each eye was dissected into 24 radial wedges. All chosen frontal sections were stained with 2% osmium tetroxide and 1.5% potassium ferrocyanide for 2 hours, *en bloc* stained with 2% uranyl acetate for 90 min, dehydrated in an ascending series of ethanol and propylene oxide, and embedded in Epon-Araldite.

### **2.2 Sectioning and Staining for Light Microscopy**

After tissue segments were processed into the Epon embedding mixture, excess plastic was trimmed to prepare for sectioning. Each capsule was carefully trimmed using a razor to cut away the excess hardened Epon mixture. Once the tissue segment in each capsule was exposed, the capsule was placed into a microtome (LKB Briomma). Glass knives were used to methodically cut s 3-5 microns in thick sections. This thickness was

used reveal the morphologic structures such as ESVs to be clearly displayed under light microscope.

Sectioned tissue samples were placed on microscope slides and each slide contained three sections from the same wedge. Each section was placed in a drop of distilled water on the microscope slide, and then placed on a hot plate to dry the section, causing it to stick to the microscope slide. Once dry, each section was stained using 0.1% Toluidine Blue on a hotplate for 10-15 seconds. Afterwards, the stain was washed from each section using distilled water, and then the slide was placed on the hotplate to dry again. Once this process was completed for all prepared samples, each of the sections were imaged by light microscopy.

### **2.3 Imaging**

Each of the slides were viewed using the light microscope with a Q-color 3-digit camera (Olympus). Sections that showed features such as the trabecular meshwork, aqueous plexus (AP), and episcleral veins (ESVs), were kept in a separate microscope-slide holder. If a particular section showed these features in addition to not having disparaging qualities (i.e., knife marks, tears, rips, etc.), then it was used for data analysis. For each eye, the best three images showing clear structural morphologies of the ESVs and TM were used for data analysis. The cross-sectional area of ESVs was measured using a program called ImageJ (NIH).

The distinction between ESVs and episcleral arteries was imperative for successful data collection throughout this study. To reduce error, ESVs and episcleral arteries were distinguished by their respective size, shape, the thickness of the vascular wall and smooth muscle layer of the vascular wall. Figure 2.1 below is an example of an image from this study depicting both ESVs and episcleral arteries near the scleral surface:

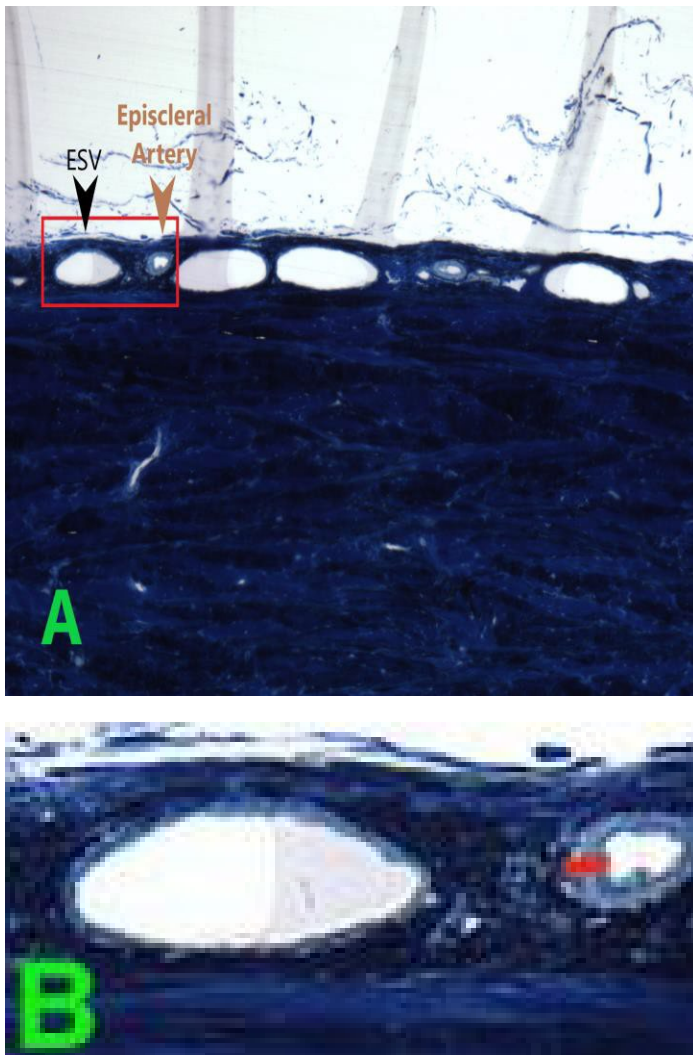


**Figure 2.1 – Representative images of ESVs and episcleral arteries**

*A. The size of episcleral veins (ESVs) (black arrow) in a porcine eye are larger than the episcleral arteries (ESAs) (brown arrow), which have a thicker smooth muscle layer around the vascular wall compared to the ESVs.*

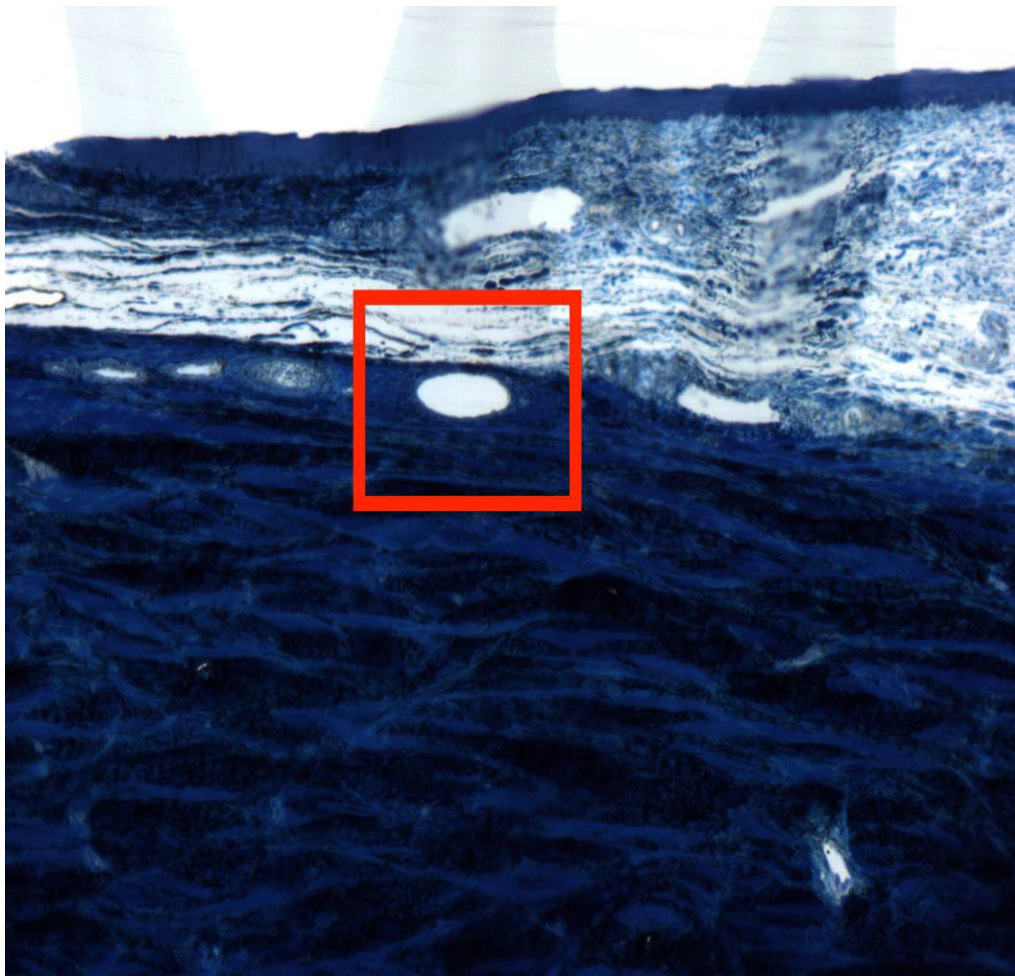
*B. The area in the red box of A at higher magnification showing an ESV and an ESA. The red line shows the thickness of the vascular wall in the ESA, which is thicker than that of the ESV.*

Figure 2.1 shows images taken from Eye #1 (wedge 4\_P1). The first image (figure 2.1A) shows the size difference between ESVs and episcleral arteries. An ESV is labelled by a black arrow and an episcleral artery by a brown arrow. ESVs are significantly larger than episcleral arteries. The second image (figure 2.1B) depicts the two blood vessels labelled in figure 2.1A at a higher magnification. The blood vessel on the left is an ESV and the vessel on the right is an episcleral artery. The main distinction between the two can be seen in the thickness of the smooth muscle layer that encapsulates each vessel. The ESV has a significantly thinner wall, whereas the episcleral artery very clearly has a thicker smooth muscle layer as indicated by the red line. Thicker walls in an artery are a physiological characteristic that is essential to the circulatory system because it allows for arteries to withstand high pressures that are needed to pump blood throughout the entire body. (Tucker et al., 2021)

## **2.4 Methods of Data Analysis**

The eyes were categorized into group A and group B without knowing which group is TSP-1 treated or control. The sections were cut from three wedges of each eye. Group A had 5 eyes, and group B had 4 eyes. Pictures were taken of the sections from three wedges of each of the eyes at 4x, 10x, and 20x magnifications. Using a program called ImageJ (NIH), ESVs were counted, and their cross-sectional areas were measured for each wedge. Every ESV was meticulously traced by hand using a tracing tool in

ImageJ, which then calculated the area within every tracing. The area of every single ESV was traced and calculated in ImageJ at 10X. Figure 2.2 below is an example of a 10x image of a sample (eye #3 – 12\_A.2) in which the ESV highlighted in red was measured for data collection.



**Figure 2.2 – An Example of an ESV from a porcine eye under light microscopy. This image was taken during data collection and depicts an ESV being identified (marked by the red box) to be measured from data collection.**

Each ESV was measured using a tracing tool within ImageJ. The tracing followed the walls of the ESVs so that the space within the tracing for each ESV was measured. This value is equivalent to the ESV area in  $\mu\text{m}^2$ .

A calibration slide was used to be able to consistently measure different images at the same distance to pixel ratio. This ensures that measuring was consistent throughout the entire process of data collection. Below was the calibration slide used to conduct data collection on ImageJ:

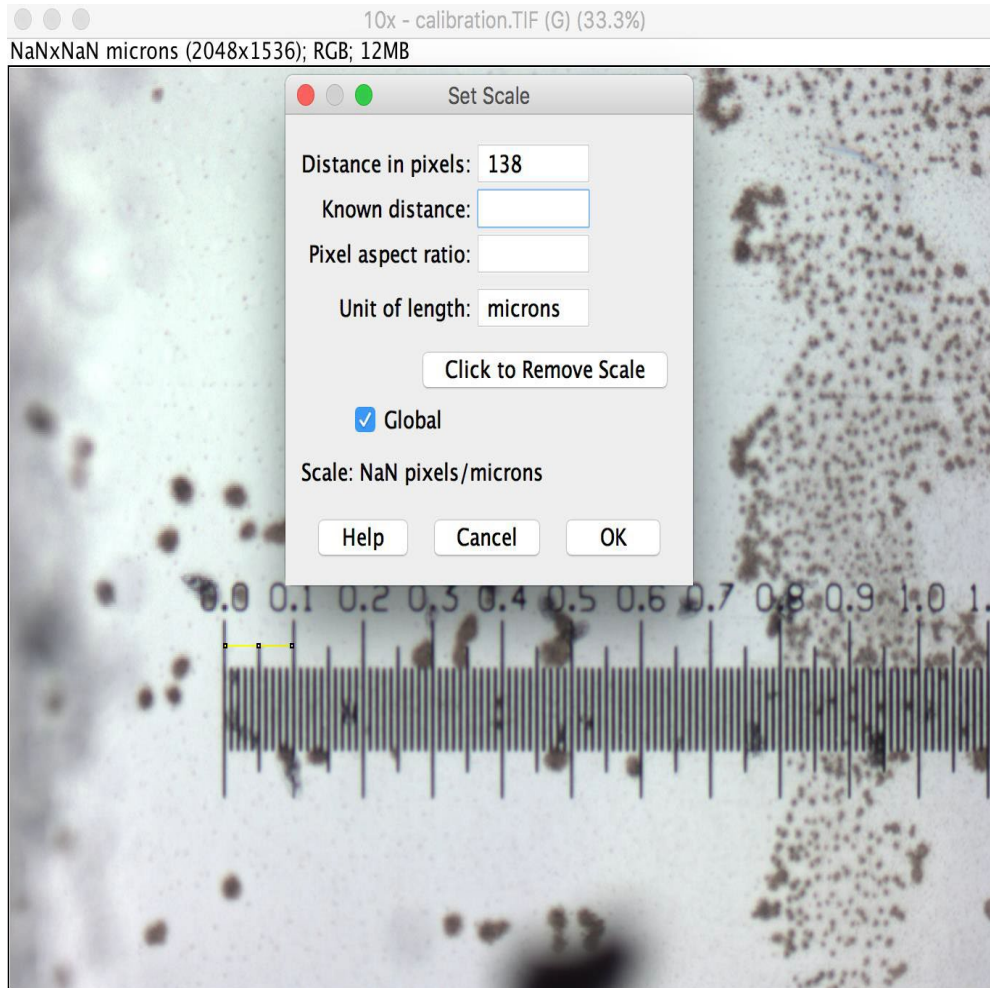


**Figure 2.3** – *Calibration slide used for ESV measurements in ImageJ. The calibration slide is used to ensure ESV measurements are consistent throughout data collection. The scale used for this study is 138 pixels:100 microns.*

For this study, based upon the calibration slide seen above, 138 pixels of the computer screen used for measurements represented 100 microns in length. Therefore, 1.38 pixels of the computer screen represented 1 micron in length. These values must be consistent throughout data collection and analysis. This reduced the chance for error

when measuring ESV areas across all eyes in this study. Figure 2.4 below shows examples of ESVs and how their cross-sectional areas were traced using the tracing tool in ImageJ:

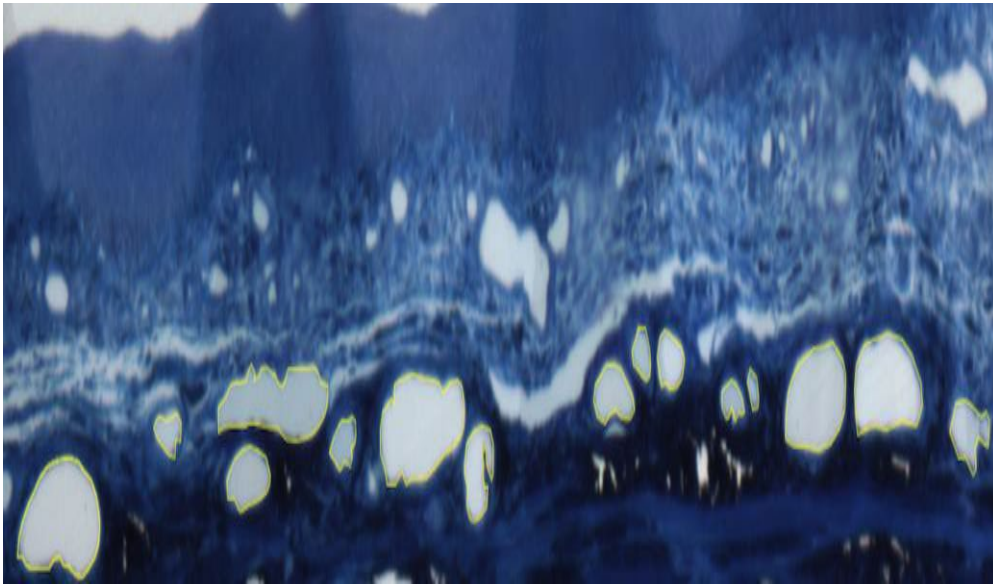


**Figure 2.4 – Example of how ESVs were traced.** This figure depicts how ESVs were traced in ImageJ to collect the cross-sectional area of ESVs. Tracings were conducted manually and are seen in the figure above (yellow outlines). ImageJ was then used to calculate the area within the tracing for each ESV.

Next, the average ESV area in  $\mu\text{m}^2$  was calculated for each of the three sections of every eye by Image J. At this point, the average ESV cross-sectional areas for a particular eye was calculated by averaging the ESV areas for **each** of the three sections from three different wedges of each eye. In addition, further statistical analyses were completed to determine a single value ( $\pm\text{SE}$ ) for the average ESV area of each of the two groups (A

and B) by conducting paired and unpaired T-tests. After all the analysis was done, the groups were decoded by Dr. Gong. Group A was control group, and group B was the TSP-1 treated group. By not knowing which group was TSP-1 treated and which group was the control until all the measurements were done, potential bias was prevented during data collection. It should be noted that ESVs that were cut obliquely on the images were excluded from data collection to reduce error in the study. Oblique cuts of ESVs contain areas that are significantly greater in size, which would cause the results of this study to be skewed if included in data analysis.

An image was taken of the TM for each of the three wedges per eye. Morphologic differences between the TMs of the control group and TSP-1 treated group was assessed. Images of the TM for each wedge were taken in 20x magnification. More specifically, the images of the TMs from each group were assessed to see if there were any noticeable differences between the two groups. In doing so, this study assessed morphologic effects of TSP-1 on ESVs and the TM.

## CHAPTER THREE – RESULTS

### **3.1 Grouping of Eyes**

The eyes were split into two separate groups: five porcine eyes treated with GBPS representing the control group, and four porcine eyes treated with TSP-1 representing the experimental group. Morphologic changes in the TM and ESVs between the TSP-1-treated eyes and un-treated control eyes were compared. The two groups were coded as Group A and Group B, so that I did not know which group of eyes were TSP-1 treated, in order to remove any bias during data collection.

### **3.2 Comparison of Average ESV Area between Control and TSP-1 Treated Eyes**

The average ESV area ( $\mu\text{m}^2$ ) between the control group and the TSP-1 treated group was calculated and summarized In Table 3.1 and Figure 3.1. First, an unpaired t-test was performed for unpaired average ESV area (N=5 in control group and N=4 in TSP1- treated group due to exclusion of one eye from treated group). Average ESV area in the TSP-1 treated group ( $797.0 \pm 30.1 \mu\text{m}^2$ ) was significantly smaller than that of the control group ( $1628.2 \pm 191.3 \mu\text{m}^2$ ) ( $P < 0.05$ ). These results suggest that TSP-1-treatment reduced ESV cross-sectional areas significantly.

(Unpaired ESV data)	Average ESV area ( $\mu\text{m}^2$ )
Control n=5	1628.2 $\pm$ 191.3
TSP-1 treated n=4	797.0 $\pm$ 30.1

**Table 3.2** –Comparison of *average ESV area between control and TSP-1 treated groups.*

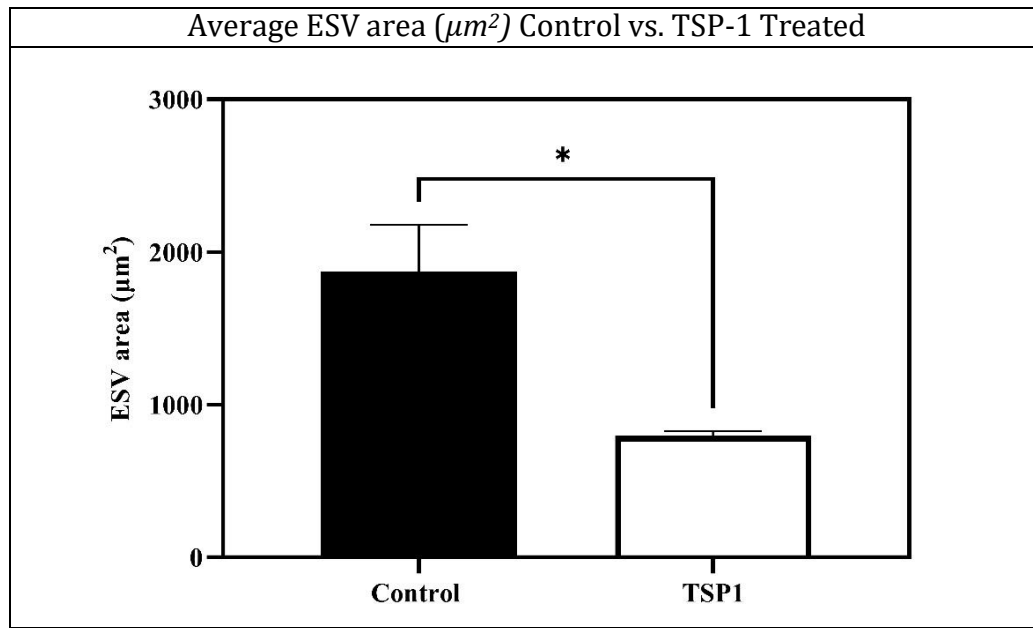


**Figure 3.1-** Unpaired t-test was performed for unpaired ESV area. *Control: n=5; Treatment: n=4. The average ESV area of the control eyes was  $1628.2 \pm 191.3$ , which was significantly larger compared to TSP-1 treated eyes ( $797.0 \pm 30.1 \mu\text{m}^2$ ). TSP-1 treated eyes demonstrated a significant reduction of  $831.2 \pm 30.1 \mu\text{m}^2$  in ESV area on average, compared to controlled eyes ( $P < 0.05$ ). Therefore, ESVs in TSP-1 treated eyes were  $51 \pm 2\%$  smaller in cross-sectional area than the control eyes*

The ESV data was then normalized to conduct a paired t-test. Four pairs of eyes were used for this analysis. Normalization of ESV cross-sectional area was completed using  $\frac{\text{Treatment}}{\text{Control}}$ . The results of the paired t-test are shown in Figure 3.2 below:

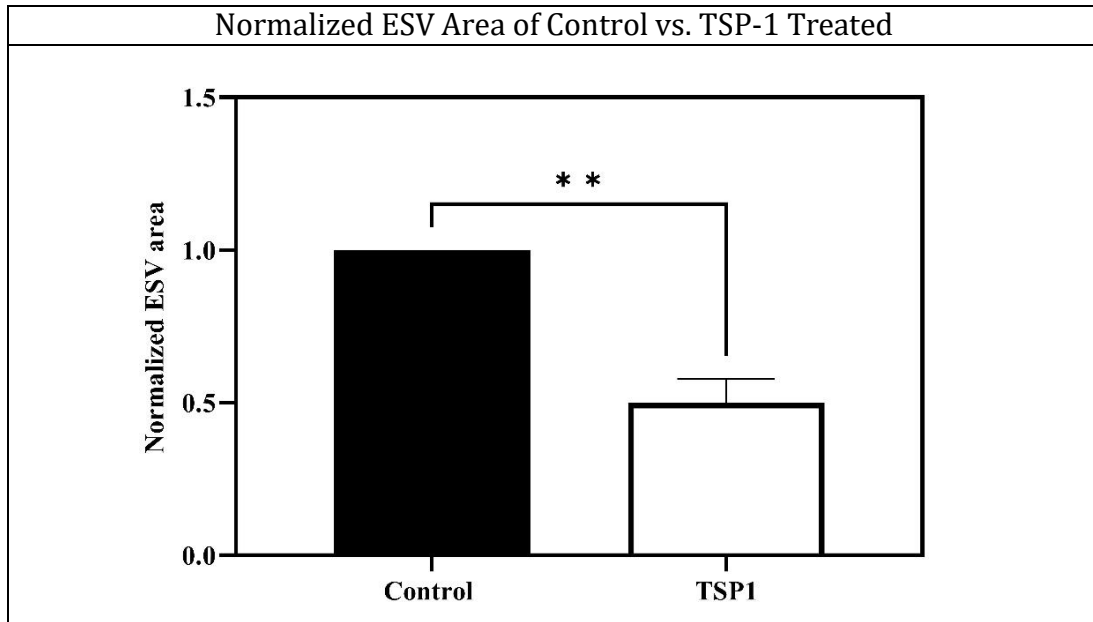


**Figure 3.2 - Paired t-test was performed for paired normalized ESV area (n=4).**

*TSP-1 treated eyes demonstrated a significant reduction of 50±8% in normalized ESV area compared to controlled eyes (P<0.01).*

Based on the results of both the unpaired and paired t-tests, the average ESV area for TSP-1 treated eyes was significantly smaller than the control eyes. Furthermore, TSP-1 treated eyes were found to have ESV areas reduced by 51±2% (unpaired t-test) and 50±8% (paired t-test). Therefore, **the TSP-1 treated eyes contained ESVs with areas that were half or less than half of the size of the ESVs in the control group.** This was calculated by:

$$\left( \frac{\text{Experimental}}{\text{Control}} \right) * 100 = \text{Percentage of Control group ESV area}$$

Results of the t-tests yielded p-values of  $P < 0.05$  for the unpaired and  $P < 0.01$  for the paired t-tests. These values were then multiplied by 100 and converted into a percentage. The p-values that were derived from the t-tests are both less 5.0%. Therefore, the data from this study showed that TSP-1 treatment decreases the size of ESVs (measured by cross-sectional area) and that this change may contribute to the decreased outflow facility found previously in TSP-1 treated eyes.

### **3.3 Comparison of Trabecular Meshwork Morphology between TSP1-treated and Control Groups**

Morphologic changes in the TM were assessed. When reviewing the TM images of each group, there were **no** noticeable or significant differences found between the TMs of the two groups. Rather, imaging showed that the TMs were similar in appearance. Furthermore, in both the control group and the TSP-1 treated group, there were no herniations or collapsed APs observed in either control eyes or TSP-1 treated eyes. Therefore, there were no significant morphologic effects of TSP-1 on the TM at the light microscopic level. A comparison of the TMs in the control (top) and TSP-1 treated (bottom) groups using light microscopy is shown below:

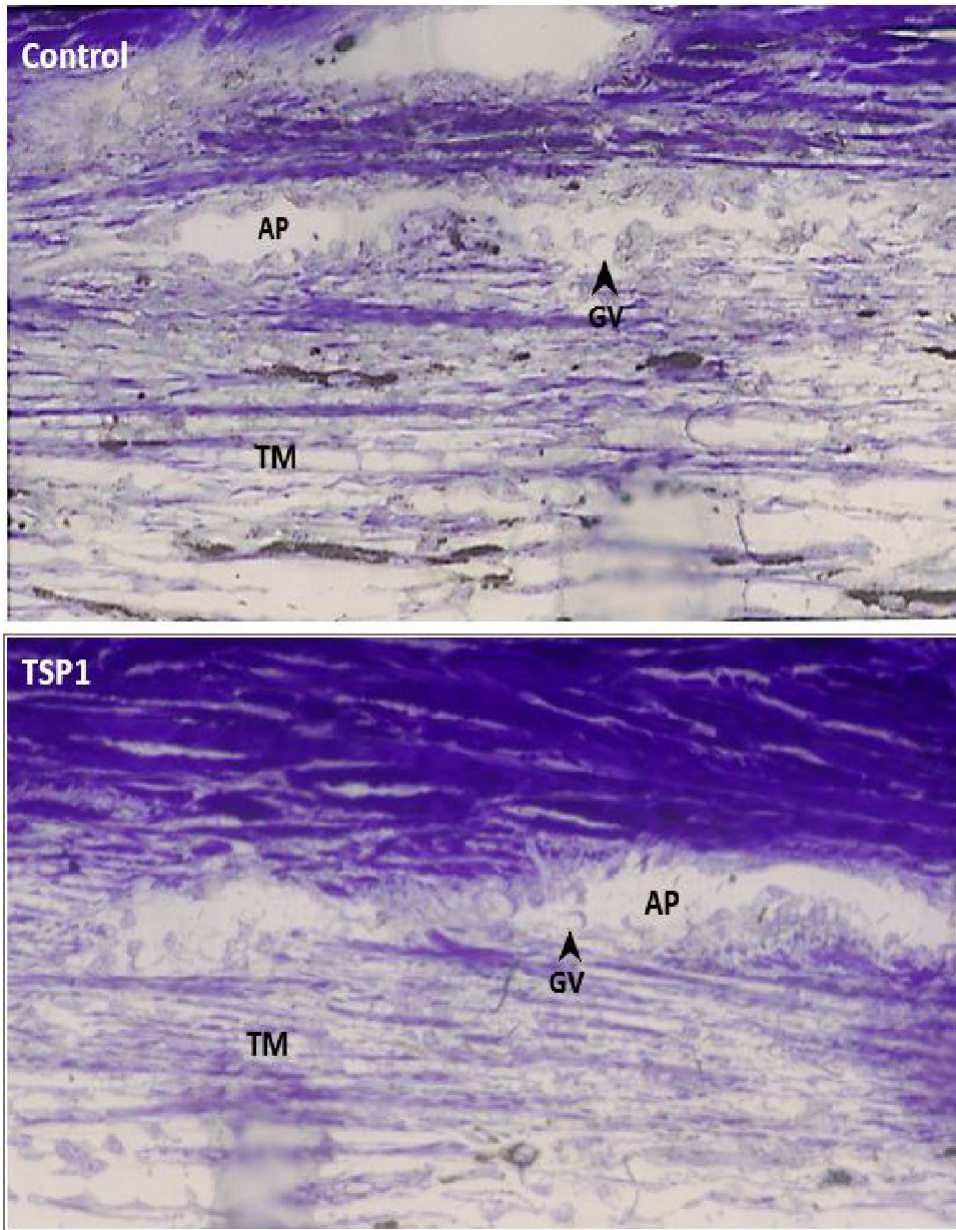


**Figure 3.3 – Comparison of *light microscopic image of the trabecular meshwork (TM), aqueous plexus (AP), and giant vacuoles (GVs) of a control eye (top) and TSP-1 treated eye (bottom) taken at 20x magnification.***

The images of the TM showed that both TSP-1 treated and control groups had similar structural morphologies. The morphological structure of trabecular beams was

visually similar in size and thickness between the groups. The inner wall endothelial cells of the AP were intact, containing giant vacuoles (GVs), and connected to the underlying cells and matrix in the juxtacanalicular tissue in both images. The morphological analysis shows that no significant difference was found between the TM of control and TSP-1 treated eyes. Since this study was a gross morphology analysis, it is possible that are changes within the TM (such as protein expression and cytoskeleton) not visible in this study that will need to be further examined.

## CHAPTER FOUR - DISCUSSION

This study assessed morphologic changes in the outflow pathways including trabecular meshwork and episcleral veins in porcine eyes that were perfused with TSP-1 using light microscopy. The main findings include:

**1) The average ESV area in eyes treated with TSP-1 were much smaller compared to those in the control group ( $p < 0.05$ , unpaired t-test,  $p < 0.01$ , paired t-test for paired normalized ESV area)**

**2) No significant morphological changes in the trabecular meshwork were observed between TSP-1 treated and control eyes.**

As a result of the reduction of the size of ESVs in the TSP-1 treated group, it can be reasoned that TSP-1 could mediate an increase in resistance to distal outflow pathway of AH. By having constricted ESVs, less AH is drained due to outflow resistance being increased. This would decrease outflow facility mediating an increase in IOP. Our findings are consistent with the previous work that showed TSP1 treatment decreases outflow facility. In addition, the effect of decreased ESV area on IOP could be explained mathematically using Poiseuille's Law assuming that AH remains consistently viscous and is a laminar flow. This law defines how fluid dynamics is related to flow rate and change

in pressure at the ends of the tube. (Rajkumar et al., 2015) Poiseuille's Law is defined by the equation:

$$\Delta Pressure = \frac{8 * \mu * L * Q}{\pi * R^4}$$

The change in pressure is related to viscosity of the fluid ( $\mu$ ), length of the pipe/vessel (L), flow rate (Q), and pipe/vessel radius (R). (Rajkumar et al., 2015) If the constriction of the ESVs were applied to this equation, then the area of the ESV correlates to the denominator of Poiseuille's Law. Therefore, if ESV area represents the denominator of the equation above and is decreased as was seen in TSP-1 treated eyes, then change in pressure increases relative to normal ESV area since the rate of AH production does not change.

The results of my study demonstrated that TSP-1 may play a role in regulating outflow facility by changing the size of ESVs. Previous findings have shown that TSP-1 is involved in the glaucoma pathogenesis because upregulated expression of TSP-1 is found in TM (Flügel-Koch et al., 2004) and lamina cribrosa cells (Kirwan et al., 2009) in glaucomatous eyes. These are two major sites of pathology in glaucomatous eyes. One study found that the IOP of TSP1-deficient mice is 10% lower when compared to corresponding wild type (WT) mice, (Haddadin et al., 2012) indicating that intraocular TSP-1 concentration may be related to IOP regulation. These suggest that **targeting TSP-1 may be a novel therapeutic approach to increase outflow facility/lower IOP.**

This study adds to current research supporting the link between TSP-1 expression and elevation of AH outflow resistance, and IOP. Previous studies have link TSP-1 to increases in blood pressure (Bauer et al., 2010), which is consistent with the findings of this study. The effects of TSP-1 on blood pressure is acting through prevention of the generation of nitric oxide (NO) and NO induced vasorelaxation of blood vessels (Bauer et al., 2010), leading to vasoconstriction and hypertension. (Bauer et al., 2010) This is a change in the size of the blood vessels mediated by TSP-1, which is consistent with the findings of our study with decreased the size of ESVs by TSP-1 treatment.

Conclusions can be made from the analysis of the data from our study. Primarily, TSP-1 induced a significant ( $P < 0.05$ ) reduction in ESV size (cross-sectional area). The reduced ESV area would be linked to an increase in resistance to AH outflow, which suggests that elevated IOP could be attributed to TSP-1 being present. Furthermore, if TSP-1 is a target for inhibition or reduction, then resistance to outflow and thus IOP could be reduced. This study did not find any significant morphologic differences in the TM in TSP-1 treated eyes when compared to the control group. These findings were based upon comparison of the light microscopical images of the TMs between TSP-1 treated eyes and control eyes. While TSP-1 is just one of the many factors that might contribute to the regulation of IOP levels, our results suggest that it could be a key target for POAG clinical research and management.

One limitation to this study was that the number of eyes used for data collection and analysis was small. There were only four TSP-1 treated eyes and five control eyes. Only four pairs of eyes were be used for paired t-test. Having a larger

sample size would strengthen the findings of this study. Although there were no morphologic differences observed between the TMs of TSP-1 treated eyes and the control eyes at light microscopic level, it is not possible to confidently state that TSP-1 does not have any impact on TM morphology. Because the TMs from each group were only compared visually for noticeable differences, quantitative analysis was not performed for the TM morphologic changes between two groups. A future study to assess morphologic changes in the TM at electron microscopic level and with a larger sample size of porcine eyes may be needed.

This study added the morphology study to prior outflow facility study in porcine eyes conducted in the Gong lab and found TSP-1 reduced the size of ESVs. The results of this study and previous studies provide us a better understanding of the potential mechanisms of TSP-1–induced reduction of outflow facility, and furthermore the role of TSP-1 in regulating outflow facility and IOP. The results of this study and previous studies suggest that by targeting TSP-1 a potential new therapeutic strategy could be developed to increase AH outflow facility and lower IOP in glaucomatous eyes.

## BIBLIOGRAPHY

- Abu-Hassan DW, Acott TS, Kelley MJ. The Trabecular Meshwork: A Basic Review of Form and Function. *Journal of Ocular Biology*. 2014 May;2(1):<http://fulltextarticles.avensonline.org/JOCB-2334-2838-02-0017.html>. doi: 10.13188/2334-2838.1000017. PMID: 25356439; PMCID: PMC4209746.
- Bauer EM, Qin Y, Miller TW, Bandle RW, Csanyi G, Pagano PJ, Bauer PM, Schnermann J, Roberts DD, Isenberg JS. Thrombospondin-1 supports blood pressure by limiting eNOS activation and endothelial-dependent vasorelaxation. *Cardiovascular Research*. 2010 Dec 1;88(3):471-81. doi: 10.1093/cvr/cvq218. Epub 2010 Jul 7. PMID: 20610415; PMCID: PMC2972685.
- Bertaud S, Aragno V, Baudouin C, Labbé A. Le glaucome primitif à angle ouvert [Primary open-angle glaucoma]. *La Revue de Medecine Interne*. 2019 Jul;40(7):445-452. French. doi: 10.1016/j.revmed.2018.12.001. Epub 2018 Dec 26. PMID: 30594326.
- Boland, Michael V. MD, PhD\* ; Quigley, Harry A. MD\*† Risk Factors and Open-angle Glaucoma: Classification and Application, *Journal of Glaucoma*: June 2007 - Volume 16 - Issue 4 - p 406-418 doi: 10.1097/IJG.0b013e31806540a1
- Borrás T. Gene expression in the trabecular meshwork and the influence of intraocular pressure. *Progress in Retinal and Eye Research*. 2003 Jul;22(4):435-63. doi: 10.1016/s1350-9462(03)00018-1. PMID: 12742391.
- Chapter 3. the glaucoma eye. Ch 3 The Glaucoma Eye. *A Patient's Guide to Glaucoma*. (n.d.). Retrieved July 7, 2022, from [https://eyerounds.org/books/glaucoma\\_guide/chapter3.html](https://eyerounds.org/books/glaucoma_guide/chapter3.html)
- Dang Y, Wang C, Shah P, Waxman S, Loewen RT, Hong Y, Esfandiari H, Loewen NA. Outflow enhancement by three different ab interno trabeculectomy procedures in a porcine anterior segment model. *Graefe's Archive for Clinical and Experimental Ophthalmology*. 2018 Jul;256(7):1305-1312. doi: 10.1007/s00417-018-3990-0. Epub 2018 May 2. PMID: 29721662; PMCID: PMC7804591.
- David L. Swain, Joseph Ho, Julia Lai, Haiyan Gong; Shorter Scleral Spur in Eyes With Primary Open-Angle Glaucoma. *Investigative Ophthalmology & Visual Science* 2015;56(3):1638-1648. doi: <https://doi.org/10.1167/iovs.14-15593>.

- Evangelho K, Mogilevskaya M, Losada-Barragan M, Vargas-Sanchez JK.  
Pathophysiology of primary open-angle glaucoma from a neuroinflammatory and neurotoxicity perspective: a review of the literature. *International Ophthalmology* 2019 Jan;39(1):259-271. doi: 10.1007/s10792-017-0795-9. Epub 2017 Dec 30. PMID: 29290065.
- Ferrer E. Trabecular meshwork as a new target for the treatment of glaucoma. *Drug News & Perspectives*. 2006 Apr;19(3):151-8. doi: 10.1358/dnp.2006.19.3.985929. PMID: 16804567.
- Fleming C, Whitlock E, Beil T, et al. Primary Care Screening for Ocular Hypertension and Primary Open-Angle Glaucoma [Internet]. Rockville (MD): Agency for Healthcare Research and Quality (US); 2005 Mar. (Evidence Syntheses, No. 34.) 1, Introduction. Available from: <https://www.ncbi.nlm.nih.gov/books/NBK42909/>
- Flügel-Koch C, Ohlmann A, Fuchshofer R, Welge-Lüssen U, Tamm ER.  
Thrombospondin-1 in the trabecular meshwork: localization in normal and glaucomatous eyes, and induction by TGF-beta1 and dexamethasone in vitro. *Experimental Eye Research*. 2004 Nov;79(5):649-63. doi: 10.1016/j.exer.2004.07.005. PMID: 15500824.
- Goel M, Picciani RG, Lee RK, Bhattacharya SK. Aqueous humor dynamics: a review. *The Open Ophthalmology Journal* 2010 Sep 3;4:52-9. doi: 10.2174/1874364101004010052. PMID: 21293732; PMCID: PMC3032230.
- Gong H, Freddo TF. The washout phenomenon in aqueous outflow--why does it matter? *Experimental Eye Research*. 2009 Apr;88(4):729-37. doi: 10.1016/j.exer.2009.01.015. PMID: 19385044; PMCID: PMC2775510.
- Gong H, Tripathi RC and Tripathi BJ: Morphology of the aqueous outflow pathway. *Microscopy Research Technique*. 33:336-367, 1996. PMID: 8652890
- Gong, Haiyan & Swain, David. (2020). Anatomy of the conventional aqueous outflow pathway. In *Current Developments in Glaucoma Surgery and MIGS*, Chapter 1, p1-37, Volume 1, January 2020 Publisher: Kugler, Amsterdam, The Netherlands. Editors: Samples JR and Ahmed IIK.
- Grewe R. Zur Geschichte des Glaukoms [The history of glaucoma]. *Klinische Monatsblätter für Augenheilkunde*. 1986 Feb;188(2):167-9. German. doi: 10.1055/s-2008-1050606. PMID: 3520122.
- Haddadin RI, Oh DJ, Kang MH, Villarreal G Jr, Kang JH, Jin R, Gong H, Rhee DJ. Thrombospondin-1 (TSP1)-null and TSP2-null mice exhibit lower intraocular pressures. *Investigative Ophthalmology & Visual Science*. 2012 Sep

28;53(10):6708-17. doi: 10.1167/iovs.11-9013. PMID: 22930728; PMCID: PMC3462480.

He, Jingna. "Pathology of Primary Open Angle Glaucoma (POAG)." Order No. 27784078 The Chinese University of Hong Kong (Hong Kong), 2019. Ann Arbor: *ProQuest*. Web. 31 May 2022.

Ivanišević M. First look into the eye. *European Journal of Ophthalmology*. 2019 Nov;29(6):685-688. doi: 10.1177/1120672118804388. Epub 2018 Oct 7. PMID: 30295065.

Kirwan RP, Wordinger RJ, Clark AF, O'Brien CJ. Differential global and extra-cellular matrix focused gene expression patterns between normal and glaucomatous human lamina cribrosa cells. *Molecular Vision*. 2009;15:76-88.

Latimer K, Pendleton C, Martinez A, Subramanian PS, Quiñones-Hinojosa A. Insight Into Glaucoma Treatment in the Early 1900s: Harvey Cushing's 1905 Operation. *JAMA Ophthalmol*. 2012;130(4):510–513. doi:10.1001/archophthalmol.2011.1184

Leffler CT, Schwartz SG, Hadi TM, Salman A, Vasuki V. The early history of glaucoma: the glaucous eye (800 BC to 1050 AD). *Clinical Ophthalmology*. 2015 Feb 2;9:207-15. doi: 10.2147/OPHTH.S77471. PMID: 25673972; PMCID: PMC4321651.

Llobet, A., Gasull, X., & Gual, A. (2003). Understanding trabecular meshwork physiology: A key to the control of intraocular pressure? *Physiology*, 18(5), 205–209. <https://doi.org/10.1152/nips.01443.2003>

Mahabadi N, Foris LA, Tripathy K. Open Angle Glaucoma. [Updated 2022 Feb 21]. In: StatPearls [Internet]. Treasure Island (FL): StatPearls Publishing; 2022 Jan-. Available from: <https://www.ncbi.nlm.nih.gov/books/NBK441887/>

McMenamin PG, Steptoe RJ. Normal anatomy of the aqueous humor outflow system in the domestic pig eye. *Journal of Anatomy*. 1991 Oct;178:65-77. PMID: 1810936; PMCID: PMC1260535.

Meyer PA. Patterns of blood flow in episcleral vessels studied by low-dose fluorescein videoangiography. *Eye (Lond)*. 1988;2 ( Pt 5):533-46. doi: 10.1038/eye.1988.104. PMID: 3256492.

Murphy-Ullrich, J. E., & Downs, J. C. (2015). The Thrombospondin1-TGF- $\beta$  Pathway and Glaucoma. *Journal of Ocular Pharmacology and Therapeutics*, 31(7), 371–375. <https://doi.org/10.1089/jop.2015.0016>

- Noecker RJ. The management of glaucoma and intraocular hypertension: current approaches and recent advances. *Therapeutics and Clinical Risk Management*. 2006 Jun;2(2):193-206. doi: 10.2147/tcrm.2006.2.2.193. PMID: 18360593; PMCID: PMC1661659.
- Rajkumar JS, Chopra P, Chintamani. Basic Physics Revisited for a Surgeon. *Indian Journal of Surgery*. 2015 Jun;77(3):169-75. doi: 10.1007/s12262-015-1308-6. PMID: 26246696; PMCID: PMC4522253.
- Ruiyi Ren, Haiyan Gong; TSP1 Deficiency Inhibits Steroid-induced IOP Elevation in Mouse Eyes. *Investigative Ophthalmology & Visual Science* 2021;62(8):2779.
- Ren, R., Li, G., Le, T. D., Kocpozynski, C., Stamer, W. D., & Gong, H. (2016). Netarsudil Increases Outflow Facility in Human Eyes Through Multiple Mechanisms. *Investigative ophthalmology & visual science*, 57(14), 6197–6209. <https://doi.org/10.1167/iovs.16-20189>
- Ruiz-Ederra, & Verkman, A. . (2006). Mouse model of sustained elevation in intraocular pressure produced by episcleral vein occlusion. *Experimental Eye Research*, 82(5), 879–884. <https://doi.org/10.1016/j.exer.2005.10.019>
- Scott PA, Lu Z, Liu Y, Gong H. Relationships between increased aqueous outflow facility during washout with the changes in hydrodynamic pattern and morphology in bovine aqueous outflow pathways. *Experimental Eye Research*. 2009 Dec;89(6):942-9. doi: 10.1016/j.exer.2009.08.002. Epub 2009 Aug 11. PMID: 19679123.
- Sihota, Ramanjit; Angmo, Dewang; Ramaswamy, Deepa; Dada, Tanuj Simplifying “target” intraocular pressure for different stages of primary open-angle glaucoma and primary angle-closure glaucoma, *Indian Journal of Ophthalmology*: April 2018 - Volume 66 - Issue 4 - p 495-505 doi: 10.4103/ijo.IJO\_1130\_17
- Stamer WD, Acott TS. Current understanding of conventional outflow dysfunction in glaucoma. *Current Opinion in Ophthalmology*. 2012 Mar;23(2):135-43. doi: 10.1097/ICU.0b013e32834ff23e. PMID: 22262082; PMCID: PMC3770936.
- Storgaard L, Tran TL, Freiberg JC, Hauser AS, Kolko M. Glaucoma Clinical Research: Trends in Treatment Strategies and Drug Development. *Frontiers in Medicine (Lausanne)*. 2021 Sep 13;8:733080. doi: 10.3389/fmed.2021.733080. PMID: 34589504; PMCID: PMC8473801.
- Tan JC, Peters DM, Kaufman PL. Recent developments in understanding the pathophysiology of elevated intraocular pressure. *Current Opinion in Ophthalmology*. 2006 Apr;17(2):168-74. doi: 10.1097/01.icu.0000193079.55240.18. PMID: 16552252.

- Tucker WD, Arora Y, Mahajan K. Anatomy, Blood Vessels. [Updated 2021 Aug 11]. In: StatPearls [Internet]. Treasure Island (FL): StatPearls Publishing; 2022 Jan-. Available from: <https://www.ncbi.nlm.nih.gov/books/NBK470401/>
- Webers, Carroll A.B., et al. "Pharmacological management of primary open-angle glaucoma: second-line options and beyond." *Drugs & Aging*, vol. 25, no. 9, Sept. 2008, pp. 729+. *Gale Academic OneFile*, [link.gale.com/apps/doc/A200671215/AONE?u=mlln\\_b\\_bumml&sid=bookmark-AONE&xid=c2feaa3d](http://link.gale.com/apps/doc/A200671215/AONE?u=mlln_b_bumml&sid=bookmark-AONE&xid=c2feaa3d). Accessed 31 May 2022.
- Weinreb RN, Aung T, Medeiros FA. The pathophysiology and treatment of glaucoma: a review. *JAMA*. 2014 May 14;311(18):1901-11. doi: 10.1001/jama.2014.3192. PMID: 24825645; PMCID: PMC4523637.
- WuDunn D. Mechanobiology of trabecular meshwork cells. *Experimental Eye Research*. 2009 Apr;88(4):718-23. doi: 10.1016/j.exer.2008.11.008. Epub 2008 Nov 24. PMID: 19071113.

**CURRICULUM VITAE**

